

Charge transport through superconductor/Anderson-insulator interfaces

Aviad Frydman and Zvi Ovadyahu

The Racah Institute of Physics, The Hebrew University, Jerusalem 91904, Israel

(Received 8 July 1996; revised manuscript received 22 November 1996)

We report on a study of charge transport through superconductor-insulator-superconductor and normal metal-insulator-superconductor structures (SIS and NIS junctions, respectively) where the insulator is of the Anderson type. Devices which are characterized by a junction resistance larger than $10\text{ k}\Omega$ show behavior which is typical of Giaever tunnel junctions. In structures having smaller resistance, several peculiar features are observed. In the SIS junctions, Josephson coupling is detected over distances much larger than the typical insulator localization length. In addition, a series of resistance peaks appears at voltages of $2\Delta/n$, where Δ is the superconducting gap. The NIS Junctions exhibit a large resistance dip at subgap bias. We discuss possible interpretations of these findings and suggest that they may result from the presence of high transmission channels through the barrier region. [S0163-1829(97)05314-9]

I. INTRODUCTION

Sufficiently strong static disorder may bring about a transition to an insulating phase in an otherwise metallic system.¹ These disorder-induced insulators, commonly referred to as ‘‘Anderson insulators,’’ differ from conventional ‘‘band insulators’’ by the fact that they have a finite, and usually large, density of electronic states $N(0)$ at the Fermi level E_F . The electronic wave functions associated with these states are confined to a region ξ , called the localization length. In a large specimen, charge transport involves hopping between localized states. Hopping is essentially a phonon-assisted tunneling, and thus, an inelastic process. On scales smaller than the characteristic hopping length r , however, quantum coherence is maintained.² At low temperature, r may become much larger than ξ and the scale over which quantum coherence is maintained may include many intermediate localized sites. This, in turn, leads to intriguing quantum-interference effects such as conductance fluctuations in small samples³ and magnetoresistance in large specimens.² A common ingredient in these phenomena is the virtual scattering from the intermediate sites that coherently contribute to the hopping probability.

In this paper we describe another type of experiment in which the physics of transport through many localized sites may play a significant role: tunneling between two metals separated by a thin Anderson insulator.

An effective way to conduct such an experiment is by using tunnel junctions between a normal metal and a superconductor (N - S) or between two superconductors (S - S). These structures are highly sensitive to the nature of the barrier separating the two electrodes. If it has a low transmission coefficient, the electric properties of the junction are governed by quasiparticle tunneling. The resulting conductance shows a dip at small bias, since single particle tunneling is forbidden within the superconducting energy gap Δ (or 2Δ in the S - S case). On the other hand, when the effective barrier is decreased so that the transmission coefficient of the junction approaches unity, the low bias conductance is dominated by Andreev reflections.⁴ These are processes that convert normal current to supercurrent in the following way: An

electron in the normal region, impinging on the interface, with energy smaller than the superconducting gap, is reflected as a hole. The missing charge, $2e$, is transferred into the superconductor as a Cooper pair. Similarly, a hole reflects from the boundary as an electron, while removing a pair from the condensate. The Andreev mechanism leads to a conductance *peak* at subgap voltages because of the double charge associated with each reflection. The transition from quasiparticle tunneling to Andreev conductivity as a function of the junction transparency T has been discussed by Blonder, Tinkham, and Klapwijk^{5,6} (BTK). They showed that a typical resistance versus voltage curve of an S - N contact exhibits a double-dip structure at $V = \pm\Delta$ due to the interplay between the two tunneling mechanisms. The precise details of this curve, in particular, the ratio between the zero bias resistance and the normal-state resistance, depend on the character of the interfacial barrier.

Recently, we presented current-voltage measurements performed on structures of these types.^{7,8} It was shown that the presence of localized states considerably enhances superconductive coupling through the junction. In the current paper we present a wide set of experimental data consistent with this notion. Most of the observed features can be explained by models for Andreev reflections by assuming the existence of high transmission through discrete channels. We explore two scenarios that may account for the appearance of such channels. One, proposed by several researchers, is based on ‘‘technological accidents’’ resulting in metallic filaments shorting out the insulating layer. The other possibility is that the channels are composed of localized sites that exist within the Anderson insulator. The merits and shortcomings of both propositions are discussed and we suggest experiments to further test them.

II. EXPERIMENT

Sample preparation

The normal metal-insulator-superconductor (NIS) and superconductor-insulator-superconductor (SIS) tunnel junction were fabricated by evaporating a thin insulating film between two metallic layers. Glass slides held at room tem-

perature were used as substrates for all the samples reported here. The insulating barriers were a -InO_x, a -Ge, or a -SiO₂, deposited by e -gun evaporation. The SiO₂ and Ge films were deposited at base pressure of 2×10^{-6} mbar at the rate of 0.5–1 Å/sec, and the InO_x layers were evaporated at a rate of 0.3 Å/sec and in an environment of $5\text{--}7 \times 10^{-4}$ mbar dry oxygen. Under these conditions,⁹ InO_x has a density of states, $N(0) = 10^{32} \text{ erg}^{-1} \text{ cm}^{-3}$. It is an Anderson insulator, as will be shown below.

The metallic films were deposited from a Knudsen evaporating source. In the NIS structures the normal electrode was Au. For the superconducting electrodes, we used Pb. The latter was chosen because it is the best studied and characterized superconductor and all its relevant parameters are known. Moreover, the critical temperature ($T_C \approx 7.2$ K) and energy gap ($\Delta \approx 1.4$ mV) of thin lead layers are fairly insensitive to these particular preparation conditions. The disadvantage is that when depositing pure Pb films, grains of lead tend to coalesce and thus result in a rough surface. It is difficult to cover such a film with a thin insulating layer without pinholes. Codepositing the Pb with 15–20 % by volume of Ag significantly improves the smoothness of the films (Fig. 1), without affecting the critical temperature or the energy gap of the layer.

Figure 2 shows atomic-force-microscope surface traces of the three insulators used in this study. Note the similarity of the surface roughness of all three. All layers appear to be continuous, with no abrupt structural modulations (that might be expected near pinholes), and have thickness variations of the order of $\pm 5\text{--}15$ Å. High-resolution TEM studies confirmed the absence of pinholes in these materials on the scale of 5 Å. On the other hand, the electric properties of these insulators are quite different. SiO₂ is a band insulator with small density of states at the Fermi energy,¹⁰ while a -Ge and a -InO_x are Anderson insulators having high $N(0)$. Figure 3 describes the low-temperature transport properties of an InO_x layer, prepared under the same conditions as those used in our junctions. The data follow the variable-range-hopping conductivity relations:

$$\ln(R) \propto \left(\frac{T_0}{T}\right)^{1/4}, \quad T_0 \propto \frac{1}{k_B N(0) \xi^3} \quad (1a)$$

in the Ohmic regime,¹¹ and

$$\ln(I) \propto -\left(\frac{F_0}{F}\right)^{1/4}, \quad F_0 = \frac{\alpha k_B T_0}{e \xi} \quad (1b)$$

for high fields.¹² Here F is the applied electric field and α is a system-dependent constant.¹³ The slopes of the curves yield the values $\xi \approx 15$ Å for the localization radius and $r = \xi(T_0/T)^{1/4} \approx 150$ Å and the hopping length at $T = 4$ K. Similar values have been reported for a -Ge (Ref. 14) [$\xi \approx 10$ Å and $r(4 \text{ K}) \approx 100$ Å].

All junctions described here are $100 \times 100 \mu\text{m}^2$. The barrier thickness d was varied in the range 70–1000 Å. In some cases, batches of four samples with different d but otherwise identical, were prepared by employing a moving shutter. The entire process of the three-layer deposition could be carried out in a single pump-down cycle by using a rotatable mask.

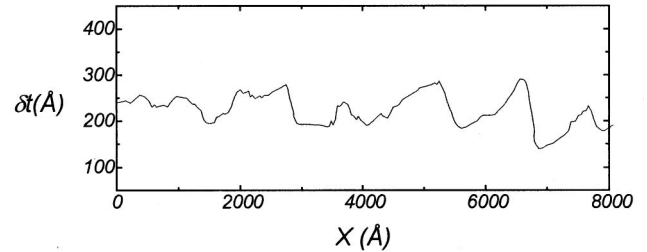
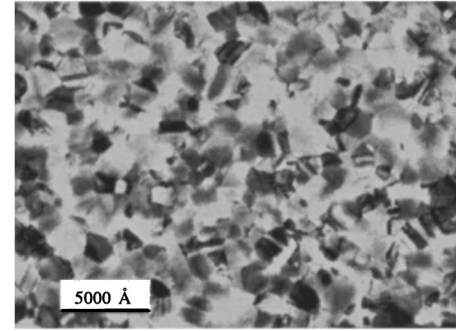
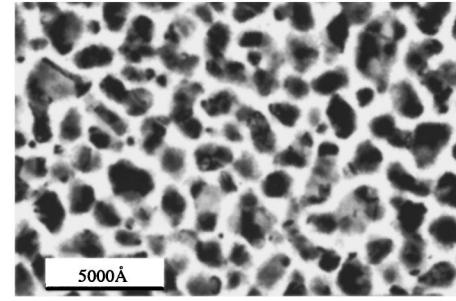


FIG. 1. TEM micrographs of a pure Pb layer having average thickness of 1200 Å (top) and of a 600 Å-thick film of Pb codeposited with Ag (middle). Bottom: Atomic force microscope line scan showing the surface roughness δt of the Pb-Ag layer. It is seen that the pure Pb film is composed of disconnected grains while the Pb-Ag layer is continuous and has thickness roughness of only ± 50 Å.

Measurement setup

The junctions were mounted in an immersion-type pumped-helium cryostat. The temperature, ranging from 4.1 to 1.2 K, was monitored by a calibrated Ge thermometer. All electric measurements were carried out by standard four-terminal methods. Current-voltage (I - V) characteristics were obtained using a Keithley 220 current source and an HP 34401A multimeter. An ac technique was used to measure the dynamic resistance versus voltage curves. This was implemented by driving an ac modulated current ramp through the sample while measuring the ac voltage drop, proportional to dV/dI , with a PAR 124A lock-in amplifier.

The cryostat was placed in the air gap of three electromagnetic Helmholtz coils with orthogonal axes. The coils in any one axis could provide magnetic fields of up to 30 Oe, while a feedback circuit, controlling the remaining two directions, could reduce ambient magnetic fields to less than 10^{-2} Oe. I - V curves in the presence of higher magnetic fields were measured in a superconducting magnet.

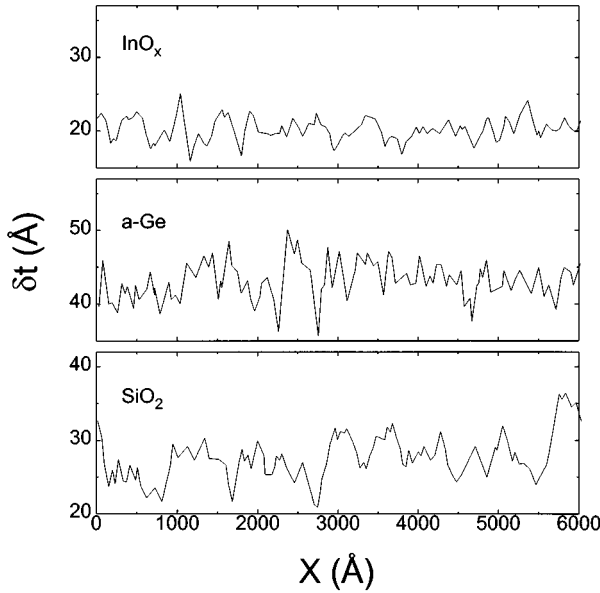


FIG. 2. Atomic-force microscope (AFM) surface traces of 200 Å-thick films of amorphous InO_x , Ge, and SiO_2 . The thickness fluctuation scale δt of the three amorphous insulators is an order of magnitude smaller than that of the Pb film in Fig. 1.

III. RESULTS

We have examined over 30 junctions of each type (NIS and SIS). Two parameters were used to characterize a sample.

(1) The barrier thickness d measured by a quartz-crystal monitor during the deposition process.

(2) The normal junction resistance R_N measured at voltages larger than the superconducting gap (i.e., for $V > 2\Delta$). The precise value of the voltage used to determine R_N is not critical. With the exception of very high resistance samples, the junction resistance changed by no more than 1% in the range 3–10 mV. (An alternative way to determine R_N would be to measure the resistance at $V=0$ while destroying superconductivity by increasing the temperature to above T_C or by applying a high enough magnetic field. However, this introduces an experimental problem. The resistance of the Pb strip, in its normal state, is often comparable to the resistance of the junction itself. Thus, if superconductivity is switched off, it is impossible to achieve true four probe measurements.)

Assuming that in a strongly localized medium the resistance increases exponentially with d ,¹⁵

$$R_N \propto \exp\left[\frac{d}{d_0}\right]. \quad (2)$$

Figure 4 shows that the experimental results can indeed be made to fit such an expression. While the average R_N and d are thus not independent, it is observed that R_N may fluctuate considerably, even for similarly prepared junctions with the same d . Such resistance fluctuations do not necessarily arise from geometrical nonuniformity in the films (such as the formation of hillocks in the Pb electrodes). Rather, they may be inherent to charge transport through thin Anderson insulators, as will be argued in the next section. It turns out that

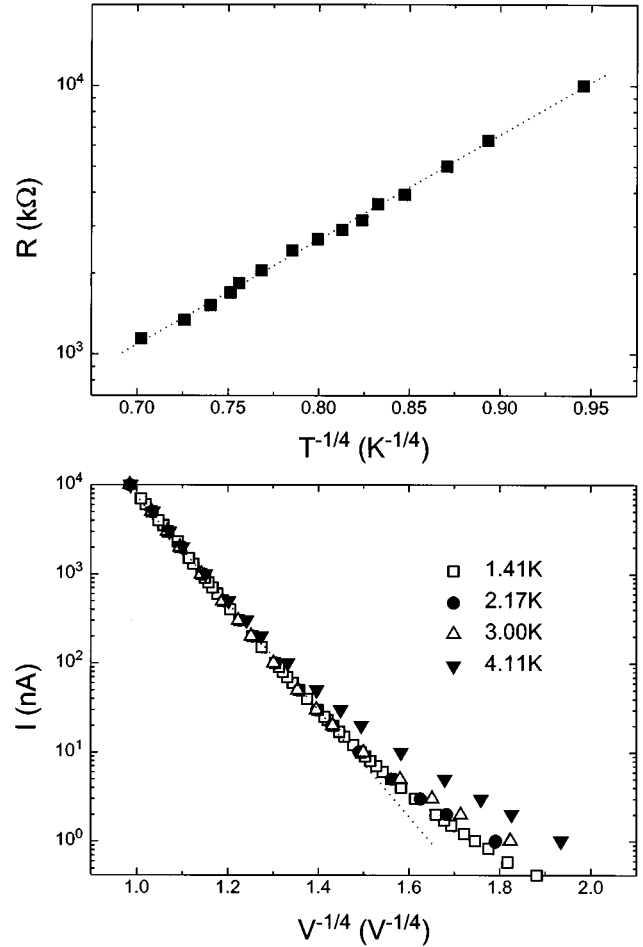


FIG. 3. Top: Resistance versus temperature of an InO_x film, 100 Å thick and 5 μm long. Bottom: Current versus voltage (I - V) curves, of the same sample, measured at different temperatures. Note that for high enough electric fields all (I - V) curves coincide and follow a $\ln(I) \propto V^{-1/4}$ -law (dotted line).

some of the observed phenomena are more sensitive to one parameter than to the other. Therefore we use both R_N and d to classify the results.

It may be argued that d_0 in Eq. (2) should be of the order of the localization length.¹⁴ From the fit presented in Fig. 4, d_0 is found to be approximately 160 Å for InO_x and 120 Å for $a\text{-Ge}$. Note that these values are an order of magnitude larger than ξ extracted from the hopping conductivity in the large samples (Fig. 3). The possible significance of this peculiarity will be discussed below.

In the following subsections, the results obtained for SIS and NIS structures are considered separately. We present the raw data of the I - V characteristics of each junction type, in particular, how they are affected by temperature and magnetic fields and how these effects depend on d and on R_N . The discussion of these results will be presented in Sec. IV.

SIS junctions

Figure 5 is a typical I - V characteristic of a SIS sample. One notes that up to a critical current I_C , no voltage drops across the junction. The I - V curve and the critical current, in

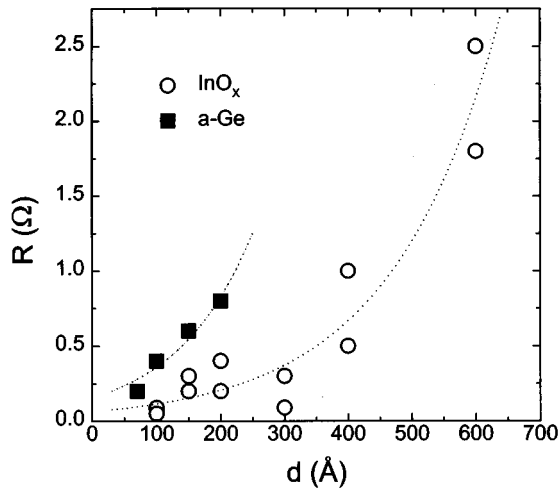


FIG. 4. Normal-state resistance, measured at $V=3.2$ mV, as a function of the barrier thickness d for a number of Ag-Pb//Pb samples where I is either InO_x or $a\text{-Ge}$. $T=4.11$ K. The dashed lines are fits to an exponential law of the type of Eq. (3). Similar results were obtained for many series of both NIS and SIS samples.

particular, depend very mildly on temperature in the range 4.1–1.2 K.¹⁶ On the other hand, applying a magnetic field has a considerable influence on the supercurrent. Figure 6 illustrates that the $I_C(H)$ dependence is typical of Josephson tunneling. Note that the interference pattern is somewhat distorted and the I_C minima do not quite reach zero. Nevertheless, the “Fraunhofer-like” nature of the plot implies that the supercurrent flows rather homogeneously through the barrier. From the oscillation period of this pattern (typically ≈ 3 Oe) one can evaluate the magnetic field penetration depth λ in the superconducting electrodes. Assuming that the current is evenly spread within the junction area, λ is found to be about 500 Å, i.e., near the expected value in Pb.¹⁷

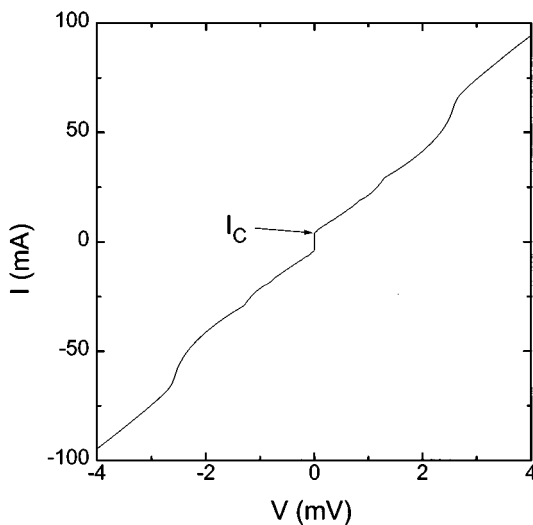


FIG. 5. Current versus voltage curve of a Ag-Pb/ InO_x /Pb junction. The barrier thickness is 150 Å and the sample resistance at $V=3.2$ mV is 0.05 Ω. Data were taken at $T=4.11$ K. The arrow marks the critical current. Note the additional structure at $0 < V < 2\Delta$ (see text).

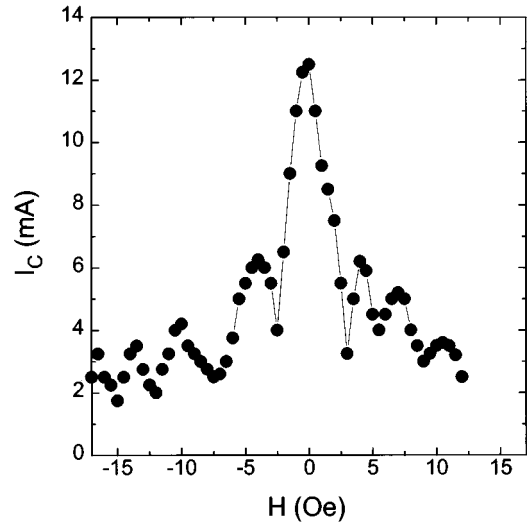


FIG. 6. Critical current magnitude of the sample presented in Fig. 5 as a function of magnetic field applied parallel to the junction layer orientation.

Figure 7 summarizes the dependence of I_C on junction parameters. These data are compared with the Ambegaokar-Baratoff¹⁸ theory for Josephson tunneling junctions:

$$I_C = \frac{\pi}{2} \frac{\Delta}{R_N} \tanh\left(\frac{\Delta}{2k_B T}\right). \quad (3)$$

It is seen that I_C is always smaller than the Ambegaokar-Baratoff prediction. The degree of this deviation is not uniform and depends on d . In samples for which $d > 400$ Å, the supercurrents are much closer to the theory than in thinner junctions where I_C is smaller by up to two orders of magnitude than predicted.

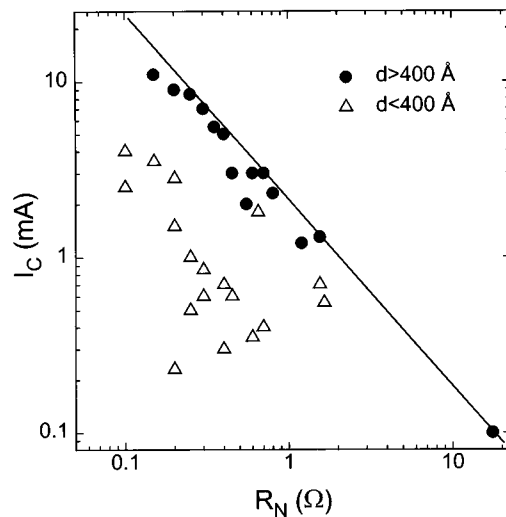


FIG. 7. Critical current as a function of the normal-state resistance for Ag-Pb/ InO_x /Pb junctions. The data are labeled by the barrier thickness range to illustrate that for large d , I_C deviates much less from the Ambegaokar-Baratoff prediction (solid line) than for samples with thin barriers.

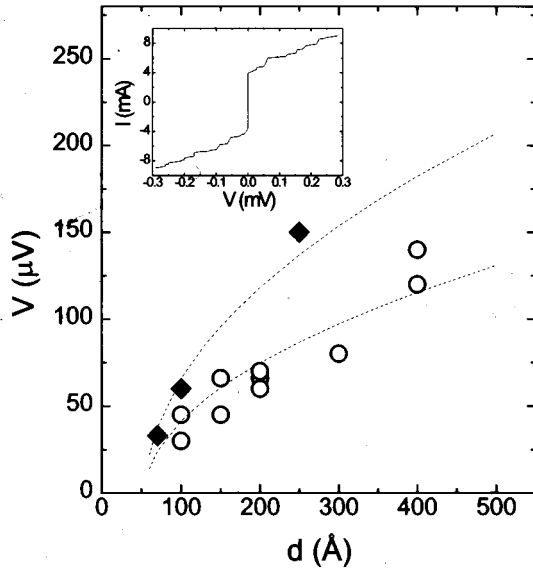


FIG. 8. The voltage quasiperiod of the current steps in several junctions (obtained from the Fourier transform of the I - V characteristics) as a function of d . The dashed lines are theoretical fits to Eq. (4). The fit was performed using $d = d_m - \beta d_m^{1/2}$, where d_m is the nominal thickness and β is a parameter. This is based on the (random) barrier-thickness fluctuations (which we directly confirmed by AFM studies of δd versus d), and on the plausible assumption that the tunneling process occurs mostly through the thinner sections. The same value for β was used for a -Ge and InO_x . Inset: typical ‘‘Fiske structure’’ for a Ag-Pb/ InO_x /Pb sample having $d = 150$ Å. $T = 4.11$ K.

When a finite bias is forced upon the junction, an additional structure is observed. This includes two types of behavior. For $V < 0.5$ mV, a series of current steps appears, as demonstrated in Fig. 8. Figure 8 also depicts this structure quasiperiod as a function of d . The details of the modulation are sample specific and, in a particular junction, they can be affected by thermally cycling the sample or by briefly subjecting it to a voltage larger than a few mV or a magnetic field larger than several Oe. For a given barrier thickness, however, the voltage quasiperiod is fixed. Such structure, customarily referred to as ‘‘Fiske steps,’’¹⁹ is a common feature of well-defined tunneling junctions and it is attributed to coupling between the ac Josephson current and the geometric resonance modes of the junction cavity. In this case, current steps are expected to occur at voltages of²⁰

$$V(n) = \frac{h}{2e} \frac{c\pi}{w} \sqrt{d/\lambda\epsilon n}, \quad (4)$$

where w is the junction width, ϵ the dielectric constant, and c the speed of light. This simple dependence on d is often used to estimate the junction barrier thickness. Inserting the insulating film thickness corrected for the surface roughness (cf. Fig. 8) in Eq. (4) yields good agreement with the measured quasiperiod.

At still higher voltages, a different modulation establishes itself. As is illustrated in Fig. 9, a series of resistance peaks are observed at voltages of $2\Delta/n$, where n is an integer. The magnitude of this modulation, A_p (defined as the peak to

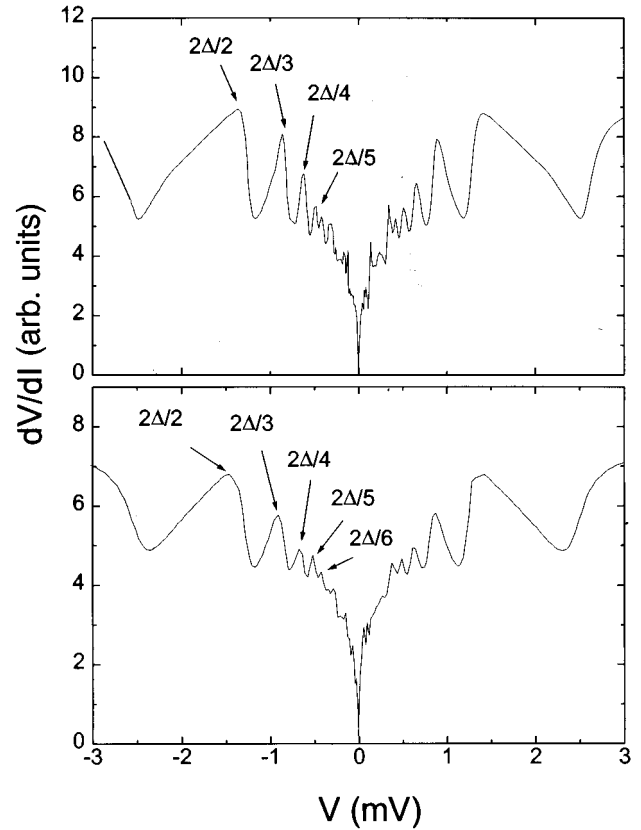


FIG. 9. Dynamic resistance versus voltage curves of Ag-Pb/ a -Ge/Pb (top) and Ag-Pb/ a - InO_x /Pb (bottom) junctions, both having barrier thickness of 100 Å. $T = 4.11$ K. The arrows mark the positions of the first few $V = 2\Delta/n$ peaks. Note the similarity between the two plots.

valley amplitude of the $2\Delta/n$ structure), weakens monotonically with n . This peak decay is more pronounced the thicker the insulating layer. Figure 10 compares the dynamic resistance dV/dI versus voltage curves of samples with different d . The dependence of A_p on n for a series of samples is shown in Fig. 11. These figures illustrate that the sub-harmonic-gap structure may be detectable up to $n = 7$ or 8 in samples with small d . When $d = 400$ Å, only the first-order peaks can be clearly identified, and when $d > 500$ Å the $2\Delta/n$ structure, including the 2Δ dips, is completely suppressed. Note, however, that the supercurrent, accompanied by the Fiske step structure, is apparent for barriers as thick as 600 Å. This is an unusual length for superconductive coupling. In conventional junctions, the Josephson effect at 1 K is suppressed by thermal fluctuations for barriers thicker than about 15 Å.²¹

The two unique features of the SIS samples, namely, the $2\Delta/n$ series and the ‘‘long-range’’ Josephson effect, were reproduced consistently in many junctions with a - InO_x and with a -Ge barriers. Unlike the Fiske steps, the sub-harmonic-gap structure is not sample specific and it maintains its shape in a large number of experimental runs or thermal cycles. However, in numerous trials with SiO_2 barriers, we were unable to measure dissipationless currents in junctions with $d > 70$ Å. For thinner barriers, a supercurrent did appear, but there the I - V characteristic exhibited a pronounced hysteresis (see Fig. 12). We suspect that this is due to metallic

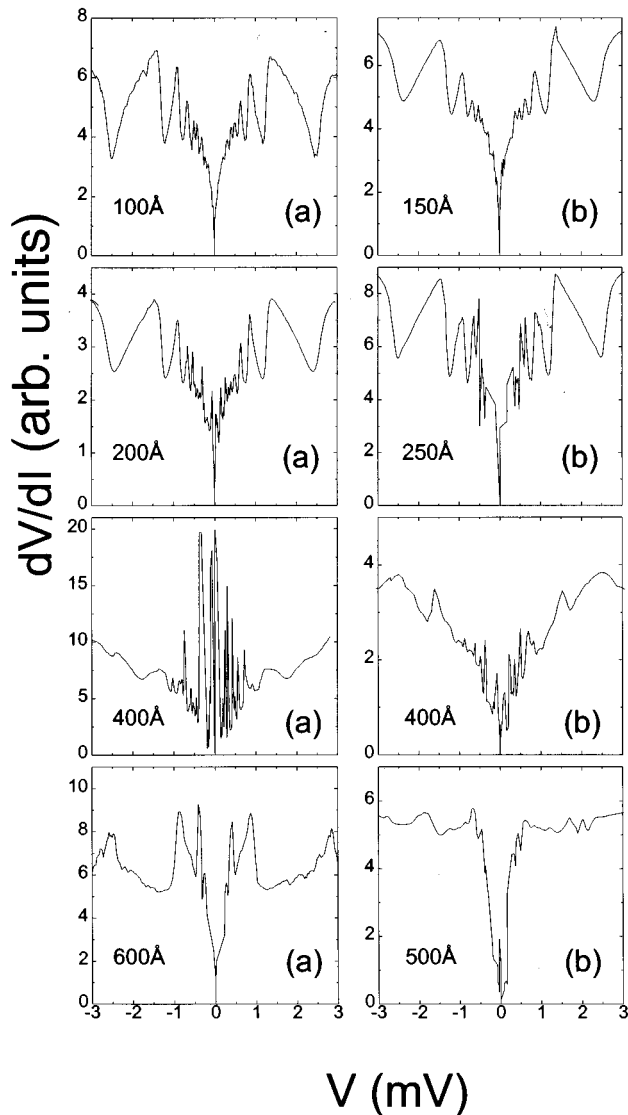


FIG. 10. Dynamic resistance versus voltage curves of two series, [(a) and (b) in the left and right columns, respectively] of Ag-Pb/InO_x/Pb samples with different barrier thicknesses. The $2\Delta/n$ series is obvious in the thin junctions, but in the thicker ones it is washed out, and the Fiske steps at small voltages become the dominant structure. Data were taken at 4.11 K.

shorts. It is significant that subharmonic-gap structure was never observed in our SiO₂ junctions.

NIS junctions

Figures 13 and 14 describe the dynamic resistance as a function of voltage for a few representative NIS samples. Though some details differ from sample to sample, the following features were observed for all junctions with $0.5 < R_N < 2000 \Omega$. A resistance dip appears at a small bias, extending up to $V \approx \Delta$. When $V > \Delta$, the junction resistance saturates at its normal-state value. The zero-bias anomaly (ZBA) depends on d . Thin junctions exhibit a very sharp resistance drop extending over a region that widens when d increases, as illustrated by Fig. 14.

Figure 15 depicts the dependence of R_0 , the resistance at $V=0$, on temperature for a series of samples. The ZBA be-

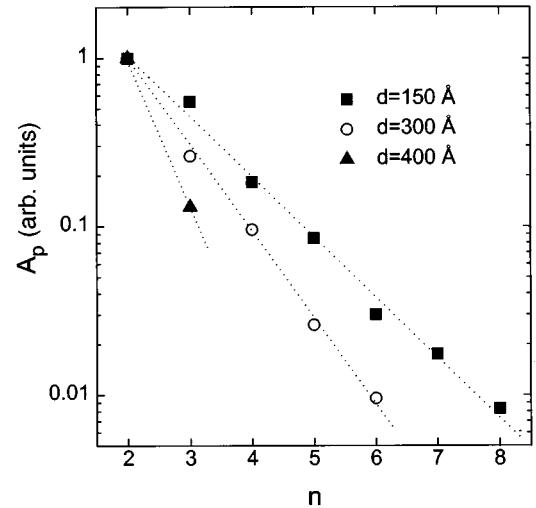


FIG. 11. Peak amplitude A_p , normalized to the $n=2$ peak, as a function of n for a series of Ag-Pb/InO_x/Pb samples having different barrier thickness. The decay of A_p is fitted to an exponential law in accordance with Eq. (5).

comes more pronounced as temperature is reduced below 4 K. This temperature dependence is steeper, the thicker the barrier. For low enough temperatures, however, R_0 tends to saturate. At $T=1.2$ K, the relative resistance drop, R_N/R_0 , reaches a typical value of 1.5–3.5. We emphasize that the characteristic voltage over which the anomaly exists is not modified by temperature, nor does it depend on R_N .

Figure 16 shows the response of the junction to a magnetic field. For $H < H_C$, H hardly affects the I - V characteristics. But as soon as superconductivity is destroyed at $H \geq H_C$, the resistance dip disappears. This establishes the role of superconductivity in giving rise to the resistance dip.

In junctions for which the resistance exceeds 10 k Ω , the I - V curves are qualitatively different. As exemplified by Fig. 17, the dynamic resistance exhibits a peak centered at $V=0$. The resistance changes, extending over a regime of voltages much larger scale than Δ . Apparently, the conductance of

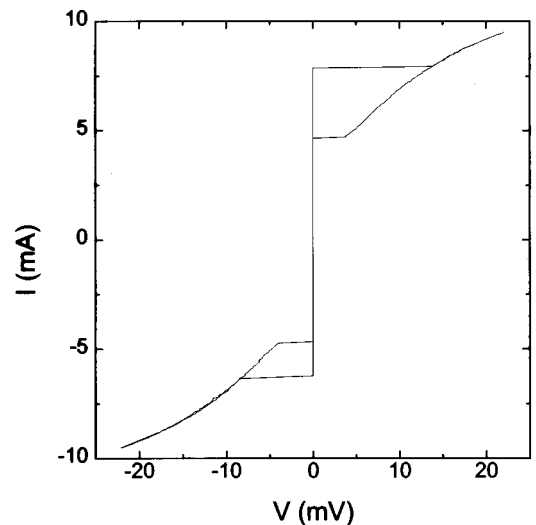


FIG. 12. Current versus voltage characteristic of a Ag-Pb/SiO₂/Pb junction. $T=4.11$ K and $d=70 \text{ \AA}$.

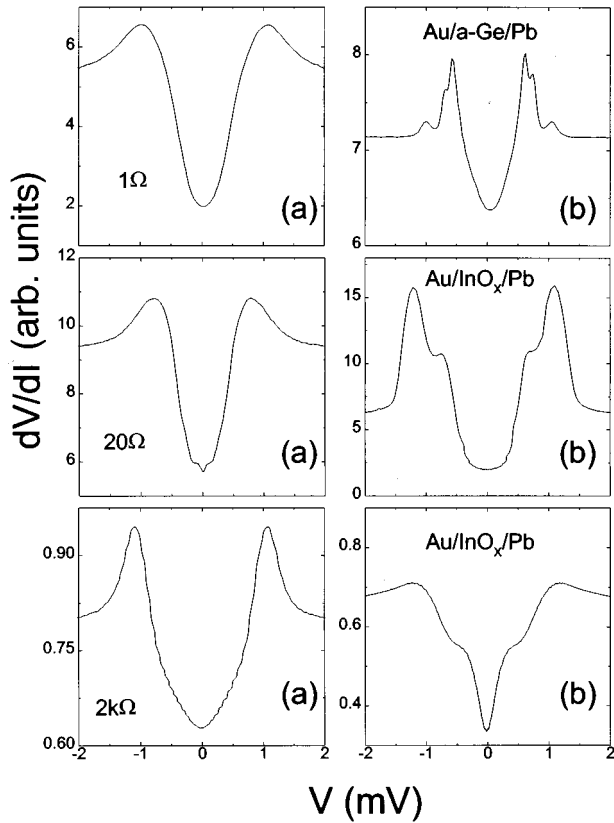


FIG. 13. Dynamic resistance versus voltage curves for several representative Au/I/Pb samples measured at $T=1.2$ K. The left column (a) shows the results of junctions which cover the normal-state-resistance range in which the ZBA is detected. The right column [marked (b)] presents samples having additional structure in the I - V curve. Note that the Ge sample exhibits a richer modulation. This is common to all a -Ge junctions.

such a junctions is highly non-Ohmic, because of inelastic hopping.^{12,13} This field-assisted hopping process overshadows all other contributions to the conductivity. However, there seems to be an additional resistance associated with the I - S interface. This can be seen from the magnetic-field dependence of the zero-bias conductivity in Fig. 17. Switching off superconductivity in the electrode causes a resistance decrease. The abrupt decrease in R occurs at H_C and correlates with the onset of resistance in the lead layer. This behavior (Fig. 16) is typical of S -to- N quasiparticle tunneling, and is just the opposite of the situation in the low-resistance samples.

IV. DISCUSSION

We begin this section by considering the experiments on the SIS junctions. Most of the features observed in these structures are characteristic of superconductive tunneling. In particular, we note the dissipationless current, its nontrivial dependence on magnetic field, and the ‘‘Fiske step’’ series, observable in Figs. 5, 6, and 8. In these regards, our samples exhibit behavior typical of conventional Josephson junctions.

The peculiar feature, which is not commonly encountered in Josephson devices, is the occurrence of the $V=2\Delta/n$ resistance peaks. This feature has been occasionally observed

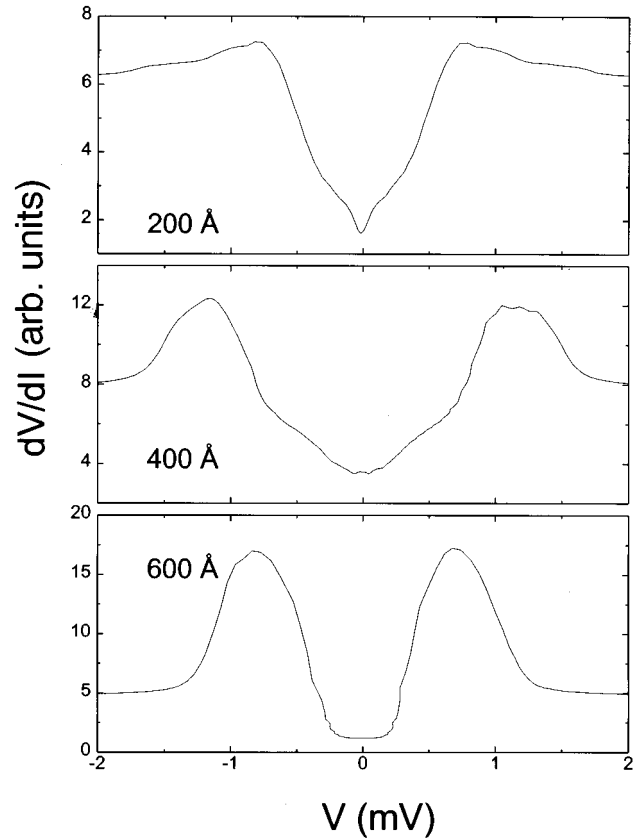


FIG. 14. dV/dI - V curve of a series of Au/InO_x/Pb samples having different d 's $T=1.2$ K. Note that the sample with the thicker barrier exhibits well-developed dynamic resistance peaks at $V \approx \pm\Delta$, implying that the low-to-normal-resistance transition occurs in an abrupt manner.

in the past,^{22,23} and its origin has been a controversial issue for several decades. The following three explanations have been suggested. (a) Absorption of an ac Josephson photon by a tunneling quasiparticle.²⁴ This mechanism leads to current

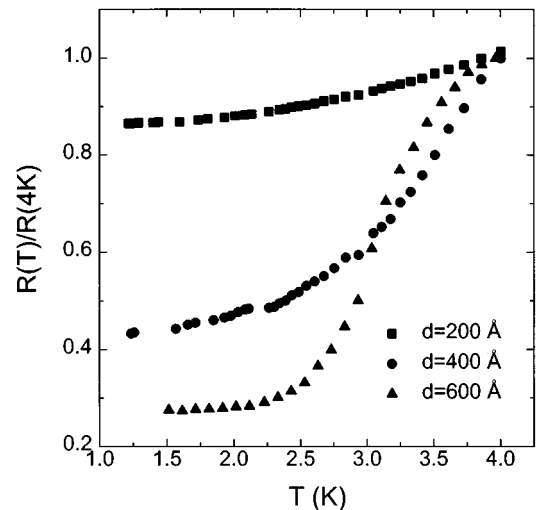


FIG. 15. Zero-bias resistance (normalized to its value at $T=4.11$ K) versus temperature for three Au/InO_x/Pb junctions with different d 's.

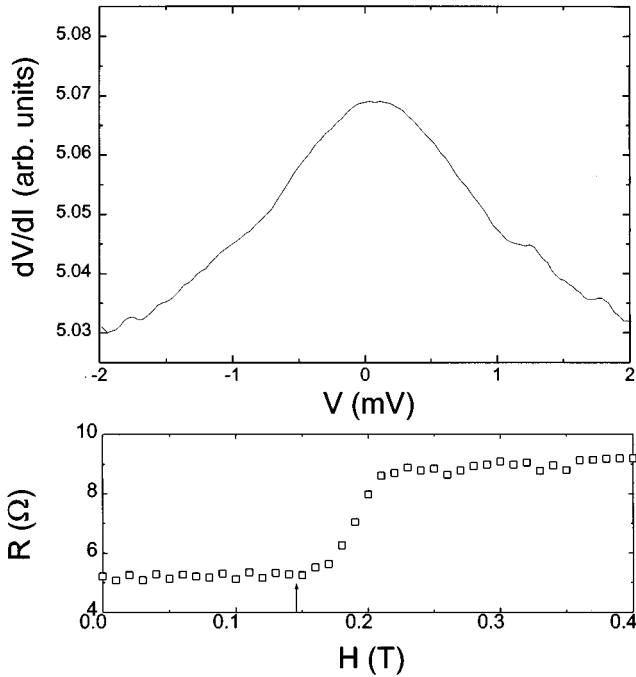


FIG. 16. Top: Dynamic resistance versus voltage for a Au/InO_x/Pb sample in the presence of a 6 T magnetic field applied parallel to the substrate to quench superconductivity. The barrier thickness is 700 Å. Bottom: The zero-bias resistance as a function of magnetic field of this sample. The arrow marks the position of the critical field of the Pb layer used as the superconducting electrode.

steps at $V=2\Delta/n$, where n is an odd integer. Another series, with even n , is related to photon absorption by the electrodes. (b) Simultaneous tunneling of n quasiparticles between the two superconductors.²⁵ (c) Multiple Andreev reflections of a quasiparticle on each of the junction interfaces.²⁶

The Josephson self-coupling mechanism described in (a) is inconsistent with our findings. It involves different processes, with different amplitudes for odd and even n . The experimental results do not reflect such a distinction between even and odd n 's. We cannot rule out the second mechanism. In the following, we attempt to explain the experimental results on the basis of the Andreev reflection mechanism, mainly because this model is detailed enough to let us deal with all aspects of our data.

Our first observation is that the $2\Delta/n$ structure is detectable for high values of n (sometimes up to $n=8$). This seems to imply that we are detecting a large number of coherent processes of particle transitions through the junction which suggests a large junction transmittance T . [This is also true if (b) is responsible for the effect.] A quantitative estimate of T can be obtained by analyzing the $2\Delta/n$ peak amplitude versus n , as illustrated in Fig. 11. If the effects we observe are due to multiple Andreev reflections, each resistance peak represents the respective contribution of the n 'th reflection, and it is presumably controlled by two factors: (1) The junction may have a smaller-than-unity transmission coefficient, i.e., some reflections are "normal" rather than "Andreev." (2) Inelastic events within the barrier destroy phase coherence. In order to obtain the "order- n " peak, the quasiparticle is

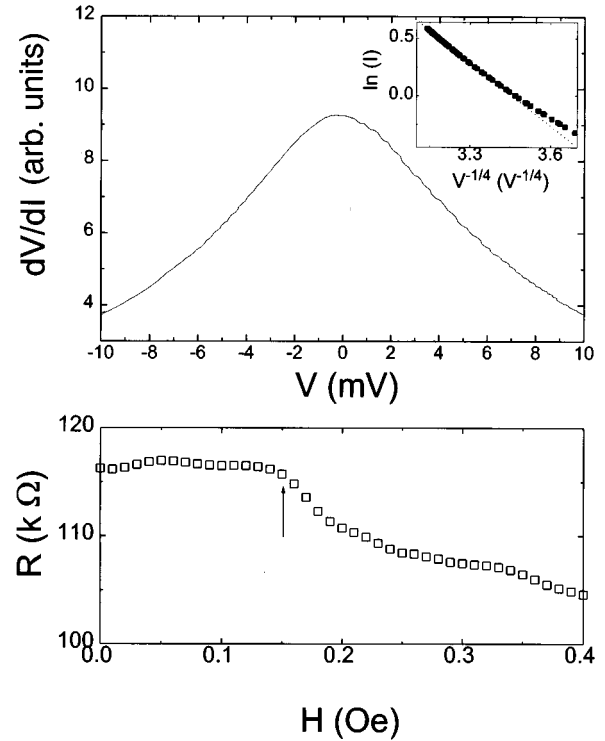


FIG. 17. Top: dynamic resistance versus voltage of an InO_x sample having a barrier thickness of 1000 Å and normal resistance of 115 K Ω . The inset shows the I - V curve extracted from these data. The observed $\ln(I) \propto V^{-1/4}$ dependence is consistent with the theoretical prediction [Eq. 1(b)]. Bottom: Zero-bias magneto resistance of the sample. The arrow marks the position of H_C . Data were taken at $T=1.2$ K.

required to travel n times across the barrier region without loss of energy or phase memory. When $n \times d$ is larger than the phase coherence length L_ϕ in the barrier, only a fraction of quasiparticles, proportional to $\exp[-n \times d/L_\phi]$ will participate in the multiple Andreev process.

Combining these two factors, the dependence of the peak magnitude on n should be

$$\ln(A_p) \approx n[\ln(T) - d/L_\phi]. \quad (5)$$

From plots of the type shown in Fig. 11, we have evaluated L_ϕ and T of many junctions.²⁷ L_ϕ is found to be about 300 and 150 Å for InO_x and Ge junctions, respectively. These values are comparable to the hopping lengths in our barrier materials. We note that quantum coherent processes exist in Anderson insulators, and the cutoff length associated with them scales with the hopping length.² This estimate, therefore, seems plausible. On the other hand, a typical value for T extracted from these analyses is 0.5–0.6. This is rather high in comparison with common tunnel junctions in which the value for the transmission coefficient is estimated²³ to be $\approx 10^{-10}$.

A related observation can be made by studying the experiments on the NIS junctions. In these devices the main finding is the resistance drop at low voltage, another feature uncommon in tunnel devices. In junctions with low transmission barriers, a resistance *peak* is expected at subgap voltages because of the energy gap for quasiparticle tunneling. The

occurrence of a ZBA, such as that observed in our samples, is often interpreted²⁸ as evidence for prominent Andreev processes. According to BTK,⁵ R_N/R_0 increases with T , and it should reach a factor of approximately 2 for an ideal interface. In all our samples exhibiting ZBA, R_N/R_0 is close to this ideal value, again suggesting that T must be large.

Next, we point out that, microscopically, charge transport in our devices occurs through some specific channels; the thicker the barrier, the more apparent the discreteness of this process. The main indication for that comes from studying the interference pattern of $I_C(H)$ (Fig. 6). Note that even for thin barriers, this feature is nonideal, in the sense that a finite critical current is detected at the minima of the pattern. As d is increased, the peak-to-valley magnitude is further suppressed, and for $d > 400$ Å, the interference part in $I_C(H)$ is essentially washed out. We recall that the quality of the interferencelike dependence of I_C on H is usually related to the homogeneity of the Josephson current across the junction. The above finding therefore implies that transport occurs rather uniformly through our thin barriers, but as d increases, the current flow becomes progressively less homogeneous. In conjunction with the previous conclusion of large T , this behavior is consistent with the following. (a) Current flows in the junction through distinct regions in space where the tunneling probability is unusually high. (b) The number of these favorable channels decreases as the barrier thickness is increased, so the current is less uniform when d is large.

The possibility that tunnel junctions are “filamentary” in nature was considered in the past by several workers²¹ who observed high-order $2\Delta/n$ resistance peaks in SIS devices. They encountered such junctions sporadically. Their resistance was relatively low and did not scale with the junction area. These observations led to the speculation that the junctions were threaded by metallic filaments through pinholes in the barrier.

At first sight, this could be a plausible way to interpret our data. The existence of high-transmission (metallic) trajectories might qualitatively explain the origin of the $2\Delta/n$ series in the SIS junctions as well as the ZBA in the NIS samples. In particular, it is reasonable that the frequency of finding accidental metallic shorts would decrease as d is increased. However, closer consideration of the data reveals several difficulties with this interpretation. For example, the inherent assumption of *accidental* occurrences of technical defects, is difficult to reconcile with the *systematic* way the features arise in a -Ge and in InO_x barriers, but not in SiO_2 barriers, although all aspects of microstructure and morphology of these films are essentially indistinguishable (cf. Sec. II). Thus there is no clue why SiO_2 should be less prone to accidental structural faults than the other two materials. (Further difficulties with the notion of “metallic filaments” will be discussed below.)

While the structural properties of all these types of barriers appear to be similar, there is a vast difference between the *electrical* properties of SiO_2 versus those of the other two. SiO_2 is a *band* insulator, and the others are Anderson insulators with a large density of states at the Fermi energy. On this basis, an alternative approach has been proposed,⁸ suggesting that the origin of “filaments” is an inherent property of Anderson-type insulators.²⁹ Such a conjecture follows from ideas first raised by Lifshitz and Kirpichenkov.³⁰ (LK),

which showed that resonant passage of electrons in a disordered system may occur via special configurations of electronic states. The presence of localized sites in a junction barrier can give rise to high transmission paths through the insulator. These trajectories are perfect quantum channels in the sense that each of them has a conductance of the order of $G_0 = e^2/h$ (and a transmission coefficient close to unity). The presence of these resonances can be expected to govern the electric behavior in both the normal and superconducting states.³¹ Thus, the junction transport is essentially determined by the probability of finding such trajectories. This probability depends on some particular properties of the insulator such as the density of states and the localization length, as well as on the junction geometry. Following this line of reasoning, Aslamasov and Fistul³² calculated the critical Josephson current through a medium containing LK resonances and obtained the following expression:

$$I_C \propto \exp\left[-\frac{d}{d_0}\right], \quad d_0 = \left\{ \xi \frac{\ln[N(0)\xi^3]}{\ln[\pi T/2(V - E_F)]} \right\}, \quad (6)$$

where V is the band energy. Inserting the relevant parameters⁹ [$E_F \approx 0.2$ eV, $V \approx 3$ V, $\xi \approx 10$ Å, $N(0) \approx 10^{32}$ erg⁻¹ cm⁻³] of our InO_x samples into Eq. (6), one finds $d_0 \approx 8-10 \xi$. A characteristic scale in our junctions should then be approximately 120–150 Å. Note that this is comparable to the scale discussed in Sec. III. The exponential increase in resistance as a function of d could well be associated with the probability of finding resonant paths in our junctions. The data in Fig. 4 are, therefore, consistent with the premise that LK resonances play an important role in the transport properties of thin Anderson insulators. Furthermore, the scatter observed in R_N versus d (Fig. 4) is a natural consequence of the statistical picture underlying this approach.³³

The basic assumption of the above hypotheses is that it is necessary to have at least one high transmission path in order to account for the peculiar transport phenomena. Hence, the total junction conductance has to be at least e^2/h . On the basis of this logic, the characteristic “crossover” resistance of 10 kΩ may not be coincidental. When $R_N \ll h/e^2 \approx 10$ kΩ, the conductance is much larger than G_0 , and many resonances could exist in the junction. At the other limit, $R_N \gg 10$ kΩ, the conductance is smaller than G_0 , and there cannot be a single high transmission channel that would give rise to resonant tunneling. A qualitative change in behavior at R_N of this magnitude is a logical corollary of this physical model.

As noted in the previous section, both the supercurrent magnitude and the ZBA width could be affected, in some special manner, by the barrier thickness. We propose a possible interpretation for such behavior in which these two results may be related. This is based on a recent work by Aleiner, Clarke, and Glazman,³⁴ who studied resonant tunneling between a superconductor and a normal metal via a single-site or double-site chain. These authors showed that a resistance drop is caused by Andreev conductivity at small bias. As the voltage is increased, the energy difference between the electron and the Andreev hole becomes larger than the resonance width Γ and the level cannot provide a large tunneling coefficient for the pair. This leads to a rise of resistance at voltages larger than Γ . As the barrier thickness is

increased, the dominant mechanism of transport shifts from resonant tunneling via a single state to trajectories which are composed of two localized sites. As a result, the resonance width Γ is broadened and the voltage dependence of the resistance becomes weaker. These calculations were not extended beyond the case of a two-state resonance, but it seems plausible that the trend will persist in chains involving three and more localized sites. If so, the widening of the ZBA feature observed when d increases may be attributed to the fact that thicker barriers are characterized by chains which contain a larger number of states. Similar considerations may be used to elucidate the results of the critical current amplitudes. In the thin barriers, the resonance is very narrow, and hence, the supercurrent can be expected to be sensitive to small fluctuations. Any small perturbation may push the system out of resonance and decrease the critical current. Thick junctions, in which the resonances are broader, are more immune to “noise,” and I_C in them is closer to the Ambegaokar-Baratoff values. This may qualitatively account for the findings in Fig. 7.

Quantitatively, however, there are several problems with the LK picture. In several NIS junctions, the ZBA magnitude R_N/R_0 was found to be as large as 3.5 (c.f. Fig. 14). If the resistance drop is due to Andreev processes, it is hard to understand such an effect. BTK predict a maximum factor of 2 for a perfect-transmission interface. According to Aleiner, Clarke, and Glazman,³⁴ a more realistic estimation for R_N/R_0 , in a strongly localized system, should be even less than this value (about 0.27). It should be noted, however, that for determining the ZBA amplitude, we compare the resistance at zero bias with that at $V > \Delta$. Thus, the normal resistance in our case is measured at high bias. This may differ from the theoretical R_N , which is defined as the zero-bias resistance in the junction normal state.

Another issue that has to be addressed is the fact that our barrier is a strongly localized medium. Such a system lacks electric screening, and the validity of resonant tunneling processes of more than one particle through such a medium should be examined more carefully. Several groups have addressed this question. Glazman and Matveev³⁵ argued that resonant tunneling of a Cooper pair is possible (and even enhanced by repulsive electron interactions), provided the width of the resonance Γ is comparable to the pairing energy $e\Delta$. Golub³⁶ has extended this idea and showed that under these conditions, Andreev mechanism in a hopping system is feasible.

The difficulties that arise in applying the LK model to the problem are not resolved by resorting to the “metallic filament picture.” If the filaments are strictly one dimensional, they, too, lack electric screening. A coherent passage of two electrons through a point contact is no more understandable than the same process via a localized state. An attempt to explain the observations using a macroscopic metallic filament (which is bound to occur occasionally if the filaments are due to random accidental faults) can be shown to be internally inconsistent with the $2\Delta/n$ data. To see that, consider a metallic wire of length L , cross section A , and resistivity ρ connecting the two superconductors. In order to observe the $2\Delta/n$ structure, a voltage of the order of Δ has to be maintained across the junction. At the same time, the current driven through the filament, $I = \Delta A / \rho d$, must not exceed the

critical current of the bulk superconductor, otherwise there would be no Δ to affect the Andreev process. This yields the following restriction on the resistivity of the filament:

$$\rho \gg \Delta / L J_C, \quad (7)$$

where J_C is the superconducting critical current density. Inserting our junction parameters $\Delta \approx 10^{-3}$ mV, $J_C \approx 10^5$ A/cm², and $L \approx 100$ Å, one obtains $\rho \gg 1$ Ω cm which is much larger than a metallic resistivity that can be reconciled with any of the materials involved.

We argue, then, that neither microscopic metallic wires nor macroscopic metallic bridges can explain our results. Actually, it is hard to see how such an explanation could be provided by the presence of any kind of a *metallic* filament. The transmission coefficient of an *S-N* contact is usually found to be quite small.⁶ This is, presumably, because of a mismatch between the Fermi wave functions of the two materials. A large ZBA is never detected in interfaces between superconductors and clean metals. Also, we are not aware of any SNS junction (N being a normal metal) in which subharmonic-gap structure has been reported, nor of an experiment where a metallic wire was deliberately placed between two superconductors and the entire set of results described above was observed. In experiments performed on “Dayem bridges,”³⁷ a subgap modulation was observed only for temperatures close to T_C .³⁸ At $T \ll T_C$, however, a clear $2\Delta/n$ structure never appeared in these systems.

In addition, we note that if the resistance measured in the NIS samples was due to the existence of metallic contacts, the temperature dependence of the ZBA ought to have looked quite different than that actually observed. Rather than a resistance that saturates at roughly half T_C (Fig. 15), one expects a systematic decrease of R_0 as the temperature is lowered due to proximity effects. There is no reason why R_N/R_0 cannot then reach values orders of magnitude bigger than 2. The total absence of such a signature in as extensive a study as ours, including dozens of different samples, weighs heavily against this picture.

In summary, we have presented measurements on tunnel junctions of SIS and NIS types, where I is an Anderson insulating material. The *I-V* curves of these structures were interpreted using Andreev reflections models. The analysis of the data indicate that these structures are threaded by regions that present much higher transmittivity than the average. We have considered two possible lines of explanations for such behavior; both assume the presence of special trajectories embedded in the insulating barrier. The first line is based on accidental penetration of metallic regions through pinholes in the insulator. The other invokes the existence of resonant channels through chains composed of localized states. It was argued that the notion of metallic filaments (although it cannot be ruled out) does not provide a satisfactory explanation for our observations. Besides being inconsistent with several empirical findings, such a model is hard to reconcile with the systematics of the results in Anderson insulator junctions as opposed to their absence in band-insulating devices. The existence of resonant trajectories naturally accounts for such a distinction, and it seems to be in agreement with most of the observations. There is still a lot to be done experimentally to further decide between the two scenarios. The corollary of the LK approach is that the

effects described here should be *universally* observed in all Anderson insulators (excluding, perhaps, materials where spin-flip interactions or other pair breakers are present). This is a strong prediction that can and should be checked. The “metallic-filament” conjecture is also amenable to a direct experimental verification: Present *e*-beam lithography techniques make it feasible to fabricate an artificial metallic filament connecting two superconductors and study its transport properties in an unambiguous way. Such experiments will be very useful in elucidating the questions raised in this work.

Finally, we remark that the main unresolved problem is the role played by Coulomb interactions in resonant tunneling processes in particular and in Andreev reflections in gen-

eral. Despite the considerable effort made by a number of researchers, this issue remains difficult and controversial. Further progress in this field seems to hinge on a much more detailed theoretical understanding of these questions than that available today.

ACKNOWLEDGMENTS

We gratefully acknowledge illuminating discussions with Y. Imry, B. Laikhtman, and M. Pollak. One of us (A.F.) wishes to thank the Charles Clore Foundation for financial support. This research has been supported by the Israeli Academy for Sciences and Humanities.

- ¹P. W. Anderson, Phys. Rev. **109**, 1492 (1958).
- ²O. Faran and Z. Ovadyahu, Phys. Rev. B **38**, 5457 (1988), and references therein.
- ³F. P. Milliken and Z. Ovadyahu, Phys. Rev. Lett. **65**, 911 (1990); J. L. Pichard, M. Sanquer, K. Slevin, and P. Debray, *ibid.* **65**, 1812 (1990).
- ⁴A. F. Andreev, Zh. Eksp. Teor. Fiz. **46**, 1823 (1964) [Sov. Phys. JETP **19**, 1228 (1964)].
- ⁵G. E. Blonder, M. Tinkham, and T. M. Klapwijk, Phys. Rev. B **25**, 4515 (1982).
- ⁶G. E. Blonder and M. Tinkham, Phys. Rev. B **27**, 112 (1983).
- ⁷A. Frydman and Z. Ovadyahu, Solid State Commun. **95**, 79 (1995).
- ⁸A. Frydman and Z. Ovadyahu, Europhys. Lett. **33**, 217 (1996).
- ⁹Z. Ovadyahu, J. Phys. C **19**, 5187 (1986).
- ¹⁰S. K. Bahl and S. M. Bhagat, J. Non-Cryst. Solids **17**, 409 (1975).
- ¹¹N. F. Mott and E. A. Davis, *Electronic Processes in Non-Crystalline Materials* (Clarendon Press, Oxford, 1979).
- ¹²B. I. Shklovskii, Fiz. Tekh. Poluprovodn. **10**, 1440 (1976) [Sov. Phys. Semicond. **10**, 855 (1976)]; M. Pollak and I. Riess, J. Phys. C **9**, 2339 (1976).
- ¹³O. Faran and Z. Ovadyahu, Solid State Commun. **67**, 823 (1988); D. Shahar and Z. Ovadyahu, Phys. Rev. Lett. **64**, 293 (1990).
- ¹⁴M. L. Knotek, M. Pollak, T. M. Donovan, and H. Kurtzman, Phys. Rev. Lett. **30**, 853 (1972).
- ¹⁵M. Ya Azbel, Solid State Commun. **45**, 527 (1983).
- ¹⁶Note that applying a voltage of the order of 1 mV across the 100 Å barrier imposes a field of ≈ 1000 V/cm. Under these conditions the resistance becomes field, rather than temperature dependent (cf. Fig. 3 and Ref. 12). Equation (3) predicts that $I_C(T)$ should also remain constant below $T \approx T_C$.
- ¹⁷R. Meservey and B. B. Schwartz, in *Superconductivity* edited by R. D. Parks (Dekker, New York, 1969).
- ¹⁸V. Ambegaokar and A. Baratoff, Phys. Rev. Lett. **10**, 486 (1963).
- ¹⁹M. D. Fiske, Rev. Mod. Phys. **36**, 221 (1964).
- ²⁰M. Dmitrenko and I. K. Yanson, Zh. Eksp. Teor. Fiz. **49**, 1741 (1965) [Sov. Phys. JETP **22**, 1190 (1966)].
- ²¹P. W. Anderson and J. M. Rowell, Phys. Rev. Lett. **10**, 230 (1993).
- ²²J. M. Rowell and W. L. Feldman, Phys. Rev. **172**, 393 (1968); A. A. Bright and J. R. Merrill, *ibid.* **184**, 226 (1969).
- ²³A. W. Kleinsasser, R. E. Miller, W. H. Mallisonand, and G. E. Arnold, Phys. Rev. Lett. **72**, 1738 (1994), and references therein.
- ²⁴N. R. Werthamer, Phys. Rev. **147**, 255 (1966).
- ²⁵J. R. Shrieffer and J. W. Wilkins, Phys. Rev. Lett. **10**, 17 (1963).
- ²⁶T. M. Klapwijk, G. E. Blonder, and M. Tinkham, Physica **109&110B**, 1657 (1982).
- ²⁷The fact that the structure decays differently for different barrier lengths indicates that it is necessary to include a spatial dependent factor in Eq. (5).
- ²⁸B. J. van Wees, P. de Vries, P. Magnee, and T. M. Klapwijk, Phys. Rev. Lett. **69**, 510 (1992); C. W. J. Beenakker, Phys. Rev. B **48**, 2812 (1992).
- ²⁹In the early experiments (Ref. 22), the barriers were the native oxides of Pb, In, or Sn. These oxides can easily become oxygen deficient and may include a large density of localized states. It is not unlikely then, that in these junctions the barriers were Anderson insulators too. See also the observation regarding the difference between “Anderson” and “band-gap” types of insulators in results obtained using barriers made of *a*-Si versus *a*-Si:H (V. N. Gubankov, S. A. Kovtonyuk and V. P. Koshelets, Zh. Eksp. Teor. Fiz. **89**, 1335 (1985) [Sov. Phys. JETP **62**, 773 (1985)]).
- ³⁰I. M. Lishitz and V. Y. Kirpichenkov, Zh. Eksp. Teor. Fiz. **77**, 989 (1979) [Sov. Phys. JETP **50**, 499 (1979)].
- ³¹S. J. Bending and M. R. Beasley, Phys. Rev. Lett. **55**, 234 (1985).
- ³²L. G. Aslamasov and M. V. Fistul', Zh. Eksp. Teor. Fiz. **83**, 1170 (1982) [Sov. Phys. JETP **56**, 666 (1982)].
- ³³M. Raikh and I. M. Ruzin, Zh. Eksp. Teor. Fiz. **92**, 2257 (1987) [Sov. Phys. JETP **65**, 1273 (1987)].
- ³⁴I. L. Aleiner, P. Clarke, and L. I. Glazman, Phys. Rev. B **53**, R7630 (1996).
- ³⁵L. I. Glazman and K. A. Matveev, Pisma Zh. Eksp. Teor. Fiz. **49**, 570 (1989) [JETP Lett. **49**, 659 (1989)].
- ³⁶A. Golub, Phys. Rev. B **52**, 7458 (1995).
- ³⁷P. E. Gregers-Hansen, E. Hendricks, M. T. Levinson, and G. R. Pickett, Phys. Rev. Lett. **31**, 524 (1973).
- ³⁸In these experiments, the data were not consistent with the multiple Andreev reflection mechanism. Two separate series were obtained for odd and even *n*, indicative of the Josephson self-coupling model.